

On the dispersive two-photon $K_L \rightarrow \mu^+ \mu^-$ amplitude

J.O. Eeg

Department of Physics, University of Oslo, N-0316 Oslo, Norway (e-mail: j.o.eeg@fys.uio.no)

K. Kumerički

Department of Physics, Faculty of Science, University of Zagreb,
POB 162, HR-10001 Zagreb, Croatia (e-mail: kkumer@phy.hr)

I. Picek

Department of Physics, Faculty of Science, University of Zagreb,
POB 162, HR-10001 Zagreb, Croatia (e-mail: picek@phy.hr)

August 1997 (revised and corrected version)

hep-ph/9605337 v2 27 Aug 1997

Preprint BI - TP 96/08, Oslo-TP-2-96 and ZTF - 96/03
hep-ph/9605337

Abstract

We present a full account of the two-loop electroweak, two-photon mediated short-distance dispersive $K_L \rightarrow \mu^+ \mu^-$ decay amplitude. QCD corrections change the sign of this amplitude and reduce it by an order of magnitude. Thus, the QCD-corrected two-loop amplitude represents only a small fraction (with the central value of 5 %) of the one-loop weak short-distance contribution, and has the same sign. In combination with a recent measurement, the standard-model prediction of the short-distance amplitude, completed in this paper, provides a constraint on the otherwise uncertain long-distance dispersive amplitude.

1 Introduction

Even before it was measured, the $K_L \rightarrow \mu^+ \mu^-$ decay had provided valuable insight into the understanding of weak interactions. The non-observation of the $K_L \rightarrow \mu^+ \mu^-$ decay at a rate comparable with that of $K^+ \rightarrow \mu^+ \nu_\mu$ showed the importance of the GIM mechanism [1]: the invention of the charmed quark made possible the necessary suppression of the amplitude. Now, equipped with the results of the new measurements and in view of the forthcoming data, we take this important amplitude under scrutiny.

The amplitudes in a free-quark calculation [2] (Fig. 1a and Fig. 1b) represented by one-loop (1L) W-box and Z-exchange diagrams, respectively, exhibited a fortuitous cancellation of the leading-order contributions. Therefore, as shown by Voloshin and Shabalin [3], one was

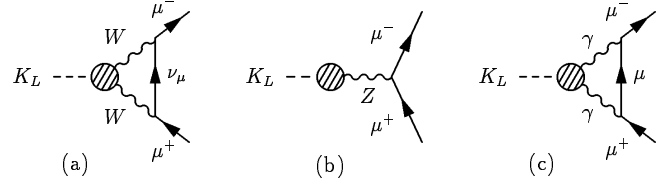


Figure 1: Possible mechanisms for $K_L \rightarrow \mu^+ \mu^-$

addressed to consider the two-loop (2L) diagrams corresponding to Fig. 1c as a potentially important *light-quark* contribution.

The contributions shown in Fig. 1c were brought to attention by the measurements [4, 5] which indicated that the *absorptive* part of the diagram in Fig. 1c dominated the rate of the $K_L \rightarrow \mu^+ \mu^-$ decay. Namely, normalizing the amplitudes to the branching ratio

$$B(K_L \rightarrow \mu^+ \mu^-) = |\text{Re}\mathcal{A}|^2 + |\text{Im}\mathcal{A}|^2, \quad (1)$$

and comparing it with the most recent BNL measurement [4]

$$B(K_L \rightarrow \mu^+ \mu^-) = (6.86 \pm 0.37) \times 10^{-9}, \quad (2)$$

exhibits the saturation by the absorptive ($\text{Im}\mathcal{A}$) part. It completely dominates the $K_L \rightarrow \gamma\gamma \rightarrow \mu^+ \mu^-$ contribution, giving the so-called unitarity bound [6]

$$B_{\text{abs}} = (6.8 \pm 0.3) \times 10^{-9}, \quad (3)$$

corresponding to $\text{Im}\mathcal{A} = 8.25 \times 10^{-5}$. Comparing the measurement (2) with the unitarity bound (3), there is room for a total $\text{Re}\mathcal{A}$ of order 2×10^{-5} . Thus, the total *real* part of the amplitude, being the sum of short-distance (SD) and long-distance (LD) dispersive contributions,

$$\text{Re}\mathcal{A} = \mathcal{A}_{\text{SD}} + \mathcal{A}_{\text{LD}}, \quad (4)$$

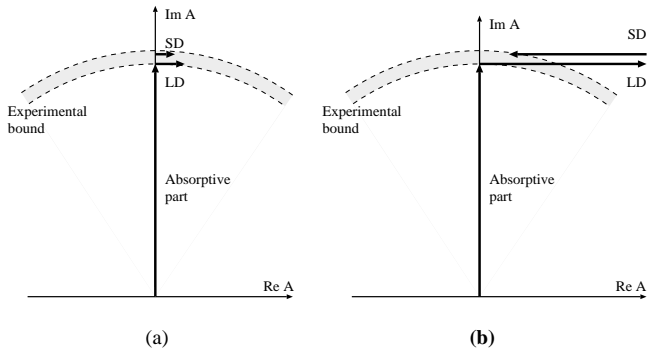


Figure 2: Schematic Argand diagram of the possible interplay of the amplitudes under consideration

must be relatively small compared with the absorptive part of the amplitude, as illustrated in Fig. 2. Such a small total dispersive amplitude can be realized either when the SD and LD parts are both small (Fig. 2a) or by partial cancellation between these two parts (Fig. 2b). Notably, the opposite sign of SD and LD contributions (as favoured by some calculations) leaves more space for an additional SD contribution. If the SD amplitude is found to be small, there is no room for a large LD dispersive amplitude \mathcal{A}_{LD} . This leads us to reconsider previous SD calculations [3, 7] in the next section.

Frequently, the SD part has been identified as the weak contribution represented by the one-loop W -box and Z -exchange diagrams of Figs. 1a and 1b. This one-loop contribution $\mathcal{A}_{1L} = \mathcal{A}_{\text{Fig.1a}} + \mathcal{A}_{\text{Fig.1b}}$ is dominated by the t -quark in the loop (proportional to the small KM-factor λ_t), and the inclusion of QCD corrections [8, 9] does not change this amplitude essentially. In the present paper we stress that the diagram of Fig. 1c ($\sim \alpha_{\text{em}}^2 G_F$) leads to the same SD operator as that of preceding two diagrams (proportional to G_F^2). As already pointed out in [3, 10], the corresponding two-loop diagrams with two intermediate virtual photons have a short-distance part \mathcal{A}_{2L} (contained in $\mathcal{A}_{\text{Fig.1c}} = \mathcal{A}_{LD} + \mathcal{A}_{2L}$) picking up a potentially sizable contribution from relatively high-momentum photons. The total SD amplitude is

$$\mathcal{A}_{SD} = \mathcal{A}_{1L} + \mathcal{A}_{2L} .$$

By exploring the contribution from Fig. 1c leading to the \mathcal{A}_{2L} amplitude, we isolate the strongly model-dependent LD dispersive piece. Section 2 is devoted to the calculation of the dispersive two-loop SD amplitude \mathcal{A}_{2L} . In section 3 we conclude that this amplitude enables us to predict the possible range of the LD dispersive amplitude \mathcal{A}_{LD} , the knowledge of which has been urged by studies of the related rare kaon decays [11].

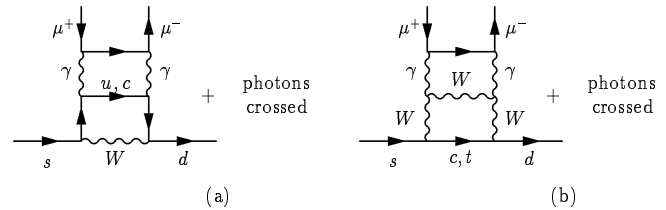


Figure 3: The dominant contributions to the $s \rightarrow d\gamma\gamma$ induced 2L diagrams: A1 for the (c, u) quarks in the loop (a); A3 for the (t, c) quarks in the loop (b)

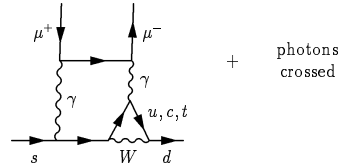


Figure 4: The dominant $B1$ contribution to the $s \rightarrow d\gamma$ induced 2L diagrams

2 Dispersive two-loop SD contribution

A complete treatment of the two-loop amplitude considered here is a missing piece in the literature. There is an enlightening feature of the diagram in Fig. 1c: the loop-momentum of the photon in Fig. 1c enables us to control the distinction between the LD and SD contributions from this diagram. We approach this problem of separating the two contributions by studying the SD piece, defined by the photon momenta above some infrared cut-off of the order of some hadronic scale Λ . A sensible SD amplitude should have a mild dependence on the choice of the particular value of Λ . We calculate the (two-loop) *quark process*

$$s\bar{d} \rightarrow \gamma\gamma \rightarrow \mu\bar{\mu} , \quad (5)$$

for which we obtain a result proportional to the left-handed quark current for the $s \rightarrow d$ transition. We present the main results of the calculation of the full set of 44 electroweak (EW) two-loop diagrams in the 't Hooft-Feynman gauge. It is convenient to distinguish between three sets of diagrams, depending on one-particle irreducible subloops – the A -diagrams given by $s \rightarrow d\gamma\gamma$ transitions (of the type shown in Fig. 3), the B -diagrams given by the $s \rightarrow d\gamma$ transition (illustrated in Fig. 4) and the C -diagrams given by the non-diagonal $s \rightarrow d$ transition (shown in Fig. 5). We stress that the $s \rightarrow d\gamma\gamma$ electroweak insertions are finite, whereas the divergent $s \rightarrow d\gamma$ and $s \rightarrow d$ insertions require a proper regularization. For the external light quarks at hand, we have used the on-shell subtraction in the limit of vanishing external 4-momenta. The structure for C -diagrams corresponds to the $s \rightarrow d$ amplitude regularized to be zero at the mass shells of the s - and d -quarks [12], in the limit $m_{s,d} \rightarrow 0$, in which we work.

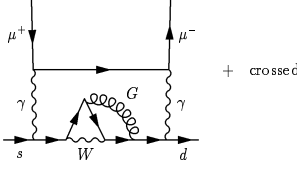


Figure 5: A genuine QCD contribution to $s \rightarrow d\mu^+\mu^-$, induced by the $s \rightarrow d$ self-penguin transition

After regularization, the effective $s \rightarrow d\gamma\gamma$ (A -transition), $s \rightarrow d\gamma$ (B -transition) and $s \rightarrow d$ (C -transition) have the structures

$$\begin{aligned} A &: \epsilon^{\mu\nu\sigma\rho} k_\sigma \bar{d}\gamma_\rho Ls, & B &: (g^{\mu\rho} k^2 - k^\mu k^\rho) \bar{d}\gamma_\rho Ls, \\ C &: \bar{d}(\gamma \cdot k)^3 Ls, \end{aligned} \quad (6)$$

where k is the photon-loop momentum (which for B - and C -diagrams coincides with the s - or d -quark momentum inside the loop). After regularization, all three types of diagrams are internally gauge invariant with respect to QED when diagrams with crossed photons are added. Other structures, besides those in (6), are present for (A) $s \rightarrow d\gamma\gamma$ and (B) $s \rightarrow d\gamma$ diagrams, but do not contribute to the two-loop quark process (5) when diagrams with crossed and uncrossed photons are summed.

The two-loop amplitude resulting from the A , B and C subloops in (6) acquires the form

$$\mathcal{M}_{2\gamma}^q = \frac{iG_F \alpha^2}{2\sqrt{2} \pi^2} \lambda_q \{A_q + B_q + C_q\} (\bar{d}\gamma^\beta Ls) (\bar{u}\gamma_\beta \gamma_5 v), \quad (7)$$

which is proportional to the same operator as that appearing in the one-loop amplitude [8, 9]. Summing over the quark flavours ($q = u, c, t$) in the loop gives us a general amplitude as

$$\begin{aligned} \mathcal{M}(s\bar{d} \rightarrow \mu\bar{\mu}) &= \sum_q \lambda_q \mathcal{M}^q \\ &= \lambda_u (\mathcal{M}^u - \mathcal{M}^c) + \lambda_t (\mathcal{M}^t - \mathcal{M}^c) \\ &= -\lambda_u \mathcal{M}^{(c,u)} + \lambda_t \mathcal{M}^{(t,c)}, \end{aligned} \quad (8)$$

explicitly exposing the GIM mechanism (the λ_q 's are the appropriate KM factors). After embedding the $s\bar{d}$ ($d\bar{s}$) in the meson \bar{K}^0 (K^0), the physical CP-conserving amplitude takes the form

$$\mathcal{A}(K_L \rightarrow \mu\bar{\mu})^{\text{CP-cons}} = -\lambda_u \mathcal{A}^{(c,u)} + \text{Re}\lambda_t \mathcal{A}^{(t,c)}. \quad (9)$$

For the light quarks ($q = c, u$), diagrams $A1$ (Fig. 3a) and $B1$ (Fig. 4) dominate completely (and are therefore under scrutiny in Table 1), the other diagrams being suppressed by an extra factor m_c^2/M_W^2 after the GIM mechanism has been taken into account. For the heavy quark (t) in the loop, such a suppression is of course absent, and we a priori have to consider all diagrams. It turns out that then the largest contribution among A -diagrams is $A3$ (Fig. 3b), and among B -diagrams the largest is again $B1$. Both in the light- and heavy-quark cases there are

also the contributions from the non-diagonal $s \rightarrow d$ self-energy (C -diagrams). Being negligible in the pure electroweak case (suppressed by m_c^2/M_W^2 for light quarks after GIM), the off-diagonal self-energy contribution becomes potentially unsuppressed ($\sim \alpha_s \ln m_c$) when perturbative QCD is switched on [13] (Fig. 5).

2.1 Pure electroweak results

Let us first display the *pure electroweak* (EW) results in order to keep contact with the early calculation by Voloshin and Shabalin [3]. We have calculated all the contributions numerically, the results of the dominating ones being presented in Table 1. In addition, the analytical expressions can be obtained in the *light-quark* (u, c) case. Let us display the analytic forms for the leading $A1$ and $B1$ amplitudes which reproduce those obtained previously [3]. Our calculation shows that, for $m^2 \ll M_W^2$, the leading logarithmic (LL) contribution in the pure electroweak case is

$$A1_{\text{LL}} = -\frac{2}{3} \left[\ln \frac{M_W^2}{\Lambda^2} - 2 \ln \frac{m^2}{\Lambda^2} \right], \quad (10)$$

where Λ is the infrared cut-off, defined above. In this way we avoid integrals over low photon momenta, which correspond to some LD contributions. For the amplitude $B1$, we obtain the following LL result for the single quark loop (for $m^2 \ll M_W^2$):

$$\begin{aligned} B1_{\text{LL}} &= -\frac{4}{9} \left[\frac{1}{2} \left(\ln \frac{M_W^2}{\Lambda^2} \right)^2 - \frac{1}{2} \left(\ln \frac{m^2}{\Lambda^2} \right)^2 \right. \\ &\quad \left. + \frac{5}{6} \ln \frac{M_W^2}{m^2} - \frac{5}{6} \ln \frac{m^2}{\Lambda^2} \right]. \end{aligned} \quad (11)$$

Taken at face value, the expressions (10) and (11) are the result for the c -quark case ($m = m_c$). The corresponding u -quark contribution is obtained by the replacement $m_u \rightarrow \Lambda$. These results conform to [3] after the GIM mechanism has been taken into account.

As a new contribution to the existing literature, we have also performed the 2L calculation of the electroweak diagrams for the *heavy* quarks ($q = t, c$) in the loop. In this case, the dominant contributions are $A3$ (Fig. 3b) and $B1$ (Fig. 4). However, these are associated with the small KM factor λ_t and are therefore suppressed. Table 1 displays only these dominant amplitudes and the total amplitudes, a full account being relegated to a more detailed publication [14]. This table also illustrates a mild sensitivity of the dominant light-quark electroweak amplitudes $A1$ and $B1$ to the IR cut-off Λ . As we have also displayed the total amplitude, this table illustrates to what degree the indicated contributions are dominant within the full set of the pure EW diagrams. The agreement between the numerical ($A1$ and $B1$) and the analytical LL results (10) and (11), after performing the GIM procedure, is explicated by the corresponding rows of Table 2. The last row of Table 1, normalized to the

measured amplitude, shows the largeness of the net EW contribution. We observe that such a large pure electroweak 2L contribution would have decreased the one loop amplitude [9] substantially.

2.2 QCD corrections

There are some subtleties in performing QCD corrections to the two-loop diagrams considered. Although the gluon corrections pertain to the quark loop, the highly off-shell photons closing the other (quark-lepton) loop control the SD regime of the two-loop amplitude as a whole. In general, there is up to one log per loop, as exemplified by the $B1$ -term in (11) related to Fig. 4.

There is a suitable prescription introduced in Refs. [8, 15] and applied by other groups [16, 17, 18] for handling the leading QCD corrections. Using this prescription, one can write the amplitude as an integral over virtual quark loop momenta. In the problem considered, we have to decode the 2-loop momentum flow in order to extract the leading logarithmic structure, which we then sum using the renormalization-group technique. Thereby, we refer to the building blocks considered previously – the electromagnetic penguin of Ref. [19] (now appearing in the $B1$ amplitude), the QCD corrections to the quark-loop of Fig. 3a [20] and to a very recent treatment of the self-penguin [21]. Let us present this in more detail.

We start by demonstrating the QCD corrections to the c - and u -quark loops of A -diagrams in Table 2. One first hunts the leading log which should correspond to the $A1$ -term in (10). This result can be understood from the result of the previous $s\bar{d} \rightarrow \gamma\gamma$ calculation [20], which consisted of two terms dominated at the scales M_W and m , respectively. Moreover, these two terms had the relative weights 1 and -2 , respectively. When this $s\bar{d} \rightarrow \gamma\gamma$ amplitude is inserted in to the two-loop diagram for $s\bar{d} \rightarrow \mu\bar{\mu}$, we gain one logarithm. Since the two terms in (10) stem from the loop integrals dominated by the momenta at M_W^2 and m^2 , respectively, the QCD-corrected amplitude acquires the form

$$A1_{\text{LL}}^{\text{QCD}} = -\frac{2}{3}\eta_1(M_W^2) \ln \frac{M_W^2}{\Lambda^2} + \frac{4}{3}\eta_1(m^2) \ln \frac{m^2}{\Lambda^2}, \quad (12)$$

which in principle agrees with [3] and disagrees with [7]. Here, the QCD coefficient η_1 reflects the colour-singlet nature of the photonic part of the diagram, and is given by

$$\eta_1(q^2) = 2c_+(q^2) - c_-(q^2), \quad (13)$$

where c_{\pm} are the Wilson coefficients of the 4-quark operators \mathcal{O}_{\pm} in the effective $\Delta S = 1$ Lagrangian of Ref. [22]. In the leading logarithmic approximation they are given by

$$c_{\pm}(q^2) = \left[\frac{\alpha_s(q^2)}{\alpha_s(M_W^2)} \right]^{a_{\pm}/b}, \quad (14)$$

where $a_+ = -2$ and $a_- = 4$ are the anomalous dimensions and $b = 11 - 2N_f/3$, N_f being the num-

ber of active flavours. In contradistinction to the numerically favourable and stable colour-octet factor $\eta_8 = (c_+ + c_-)/2$, the singlet coefficient (13) is rather sensitive to the choice of Λ_{QCD} , with a notable switch of the sign [15, 17] for q^2 at the scale of a few GeV^2 . Combining the u - and c -quark contributions by taking into account the GIM mechanism (see (8)), only the second term in (12) survives.

The $B1$ amplitude in (11) can be understood in terms of the electromagnetic penguin subloop, which is, within the LL expansion, proportional to

$$\begin{aligned} \ln\left(\frac{M_W^2}{m^2}\right) - \frac{5}{6} & \quad \text{for } k^2 < m^2 < M_W^2, \\ \ln\left(\frac{M_W^2}{k^2}\right) + \frac{5}{6} & \quad \text{for } m^2 < k^2 < M_W^2, \end{aligned} \quad (15)$$

where k is the momentum of virtual photons. Inserting this subloop into the next loop, we gain one logarithm (in particular, $\ln \rightarrow \ln^2/2$). Hence the \log^2 form in the second term in (11), which leads to the QCD-corrected amplitude expressed in an integral form as

$$\begin{aligned} B1_{\text{LL}}^{\text{QCD}} = & -\frac{4}{9} \left[\int_{m^2}^{M_W^2} \frac{dp^2}{p^2} \eta_1(p^2) \left(\ln \frac{p^2}{\Lambda^2} + \frac{5}{6} \right) \right. \\ & \left. - \frac{5}{6} \eta_1(m^2) \ln \frac{m^2}{\Lambda^2} \right]. \end{aligned} \quad (16)$$

Again, the expressions (12) and (16) apply directly to the c -quark contribution, the u -quark contribution being obtained by making the replacement $m \rightarrow \Lambda$. This means that when taking into account the GIM mechanism, the integral in (16) will run from Λ^2 to m_c^2 . The net result of the QCD dressing is similar to that for the $A1$ diagram: a suppressed amplitude with a change of sign.

The C -contribution stemming from the QCD-induced self-penguin (SP) in Fig. 5. might also be interesting. As opposed to $A1$ and $B1$ contributions it is not suppressed by the colour singlet factor η_1 , but contains the numerically favourable colour octet factor η_8 . It is, however, suppressed by α_s/π . For the $m = m_c$ case, we obtain to all orders in QCD

$$\begin{aligned} C_{\text{LL}}^{\text{QCD}} = & \frac{7}{162} \left[\int_{m^2}^{M_W^2} \frac{dp^2}{p^2} \rho(p^2) \left[\frac{1}{2} \left(\ln \frac{p^2}{\Lambda^2} \right)^2 \right. \right. \\ & \left. \left. + \left(\frac{5}{6} + \frac{25}{21} \right) \ln \frac{p^2}{\Lambda^2} \right] - \frac{5}{6} \rho(m^2) \frac{1}{2} \left(\ln \frac{m^2}{\Lambda^2} \right)^2 \right] \end{aligned} \quad (17)$$

where $\rho(p^2) = \eta_8(p^2)\alpha_s(p^2)/\pi$. In addition, $7/162$ is an overall loop factor, and the terms $5/6$ have the same origin as in (15) and (16). The u -quark contribution is again obtained by making the replacement $m \rightarrow \Lambda$.

The light-quark approximation ($m^2 \ll M_W^2$) is used in (17). For an arbitrary quark mass, needed to treat the heavy top in the loop, the calculations are much more difficult [21]. We have done an estimate and found that

Table 1: The pure electroweak light-quark (c, u) and heavy-quark (t, c) 2-loop results. The input values are $m_t=173$ GeV, $m_c = 1.5$ GeV and m_u replaced by the IR cut-off Λ of 0.7 or 0.9 GeV (corresponding to the range considered in (18)). The values in the last row are obtained by multiplying by $\lambda_u = 0.215$ or $\lambda_t \simeq 2 \times 10^{-4}$, and should be compared with $|\mathcal{A}_{\text{expt}}| \simeq |\text{Im}\mathcal{A}| = \sqrt{B_{\text{abs}}} = 8.25 \times 10^{-5}$. The one-loop (1L) SD contribution corresponds to a $\text{Re}A$ (see (19)) of the order -3.5×10^{-5}

Dominant (c, u) diagram	Pure EW		Dominant (t, c) diagram	Pure EW	
	$\Lambda = 0.7$	$\Lambda = 0.9$		$\Lambda = 0.7$	$\Lambda = 0.9$
A1	1.86	1.22	A3	23.8	22.7
A total	1.90	1.25	A total	27.1	26.4
B1	1.70	1.04	B1	20.6	19.1
B total	1.70	1.03	B total	15.6	14.2
Total	3.59	2.28	Total	42.7	40.7
Re $\mathcal{A}/10^{-5}$	1.55	0.98	Re $\mathcal{A}/10^{-5}$	0.017	0.016

the top-quark contribution is roughly 10 % of the charm-quark contribution (taking into account that α_s at m_t is about 1/3 of α_s at m_c).

Table 2 displays a detailed structure of the dominant amplitudes from Table 1, before and after applying the GIM mechanism: the first, the second, and the third block of the table display the A , B , and C contributions, respectively. In the third block, C_{LL}^{SP} and C_{LL}^{QCD} refer to the bare and dressed self-penguin contributions, respectively, whereas C refers to the negligible pure electroweak (EW) contribution. Therefore, C_{LL}^{SP} is different from C . As a curiosity, we have found that the latter has a peculiar GIM cancellation: there is an exact cancellation between the c -quark contribution for $m_c \rightarrow 0$ and the t -quark contribution for $m_t \rightarrow \infty$. As a result, C is not so GIM-relaxed as expected for a heavy-quark case (t, c).

3 Conclusions

In this paper we have focused on the 2-loop (2L) contributions, leading to the typical SD local operator for the $s\bar{d} \rightarrow \gamma\gamma \rightarrow \mu^+\mu^-$ quark transition but also having a LD (soft-photon) range. Our approach starts from the SD side, whereby an infrared (IR) cut-off of virtual photons sets in. We contrast the SD contribution with the complementary LD ones, which have to be calculated using other methods, and are rather model dependent at the present stage. The numerically important 2L *pure electroweak* SD contributions are due to the light (u, c) quarks in the loop. Besides completing the previous calculation for light quarks, we have also considered the 2L diagrams including the heavy (c, t) quarks. A large number of electroweak diagrams may compensate for a small CKM factor, and one might expect non-negligible effects. However, the actual calculation shows that the various amplitudes have different signs, and taking into account the smallness of λ_t , the heavy-quark contribution is negligible.

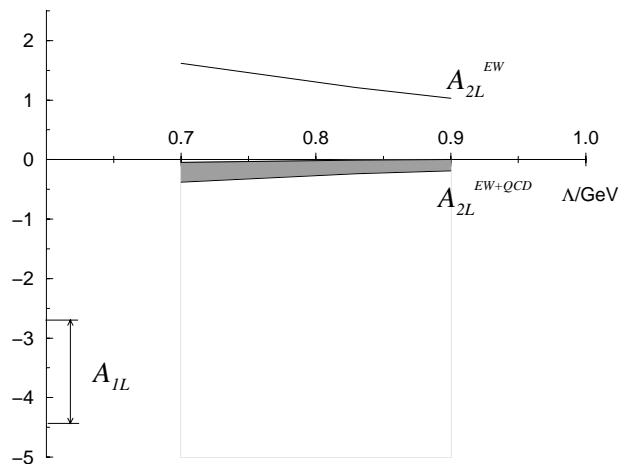


Figure 6: QCD does three things to the EW 2L amplitude:

- i) smoothens the Λ -dependence (making the SD extraction better defined),
- ii) changes the sign (making it coherent to the 1L amplitude), and
- iii) suppresses it to large extent

Next, we have shown the importance of the SD QCD corrections for the 2L diagrams, summarized in Fig. 6. Inclusion of these QCD corrections appears to be subtle and more dramatic than it was the case for the 1L diagrams. Two decades ago there was a controversy concerning QCD corrections to these 1L diagrams. Ref. [8] resolved it by an adequate treatment of the loop integrals. Our results for SD corrections to the 2L diagrams are shown in Table 2. The short-distance QCD corrections suppress the part of the SD 2γ amplitude which is electroweakly dominant before inclusion of QCD corrections. The basic reason for this is the behaviour of the $\eta_1 = (2c_+ - c_-)$ QCD coefficient. In particular, the A1 and B1 amplitudes are suppressed to a large extent,

Table 2: The anatomy of QCD corrections: the exact EW 2-loop calculation is compared with the LL values and with the RGE summed LL QCD corrections. The input values are the same as in Table 1, with the IR cut-off specified at $\Lambda=0.83$ GeV and with $\alpha_s(M_Z) = 0.118$ [23]. Correspondence with the empirical value can be made using the conversion factors provided by the last row of Table 1

	EW + SD QCD				EW + SD QCD		
	<i>c</i> -loop	<i>u</i> -loop	GIM (<i>c</i> - <i>u</i>)		<i>t</i> -loop	<i>c</i> -loop	GIM (<i>t</i> - <i>c</i>)
<i>A</i> 1	-2.14	-3.57	1.42	<i>A</i> 3	-17.4	-40.4	23.0
<i>A</i> 1 _{LL}	-4.52	-6.09	1.58	<i>A</i> 3 _{LL}	-22.3	-18.3	-4.0
<i>A</i> 1 _{LL} ^{QCD}	-6.19	-6.09	-0.10	<i>A</i> 3 _{LL} ^{QCD}	-22.3	-18.3	-4.0
<i>B</i> 1	-20.4	-21.6	1.24	<i>B</i> 1	-0.8	-20.4	19.6
<i>B</i> 1 _{LL}	-20.8	-22.0	1.19	<i>B</i> 1 _{LL}	-2.0	-20.8	18.8
<i>B</i> 1 _{LL} ^{QCD}	-14.9	-14.7	-0.23	<i>B</i> 1 _{LL} ^{QCD}	-2.0	-14.9	12.9
<i>C</i>	-0.61	-0.61	3×10^{-3}	<i>C</i>	-0.52	-0.61	0.09
<i>C</i> _{LL} ^{SP}	0.46	0.47	-0.01	<i>C</i> _{LL} ^{SP}	< 0.2	0.47	< 0.7
<i>C</i> _{LL} ^{QCD}	0.47	0.48	-0.01	<i>C</i> _{LL} ^{QCD}	< 0.2	0.47	< 0.7

and do not anymore interfere destructively with the 1L SD amplitude of Ref. [9]. Without this suppression, the scenario of Fig. 2a would appear as a more likely one.

We should stress that in the treatment of the 2L amplitude we have performed QCD corrections in the leading logarithmic approximation by using (14), while the 1L amplitude was treated in the next to leading (NLO) approximation in [9].

To summarize, we have found a modest light-quark 2L contribution stemming from intermediate virtual photons having relatively high momentum. Introducing the error bars corresponding to Λ in the range 0.7–0.9 GeV, and a more essential one from empirical uncertainty in α_s (corresponding to $\Lambda_{\text{QCD}}^{(5)}$ in the range 150–250 MeV), we obtain

$$-0.38 \times 10^{-5} \leq \mathcal{A}_{2L} \leq -0.001 \times 10^{-5}, \quad (18)$$

This has the same sign and, for central values, corresponds to 5 % of \mathcal{A}_{1L} [9],

$$-4.4 \times 10^{-5} \leq \mathcal{A}_{1L} \leq -2.6 \times 10^{-5}, \quad (19)$$

where the uncertainty mainly reflects the poor knowledge of λ_t . Although the 1L and 2L contributions are not treated on an equal footing (NLO versus LL QCD corrections), this result still enables us to estimate the size of \mathcal{A}_{LD} from (4). Referring to our comments below (3), and allowing for a $|\text{Re}\mathcal{A}| \leq 2.7 \times 10^{-5}$, we find the following allowed range for \mathcal{A}_{LD} :

$$-0.1 \times 10^{-5} \leq \mathcal{A}_{LD} \leq 7.5 \times 10^{-5}. \quad (20)$$

Thus, having a dispersive LD part \mathcal{A}_{LD} of the size comparable with the absorptive part [24] is still not ruled out completely.

The two vector-meson dominance calculations for the LD amplitude considered as the referent calculations in Ref. [4] have basically opposite signs:

$$-2.9 \times 10^{-5} \leq \mathcal{A}_{LD} \leq 0.5 \times 10^{-5} \quad [25],$$

$$0.27 \times 10^{-5} \leq \mathcal{A}_{LD} \leq 4.7 \times 10^{-5} \quad [26].$$

On the basis of the inferred relative sign between 1L and 2L contributions, Ref. [7], attempted to discriminate between the two LD calculations quoted above. (They favoured Ref. [25], and disfavoured Ref. [26] as the one ascribing opposite signs to SD and LD.) In the last of their papers [7] they even concluded that the BNL measurements [4] were in conflict with the standard model.

We have found that these conclusions are doubtful, since they are based on an erroneous SD extension to the LD momentum region. In our opinion, Ref. [7] misidentifies what (according to the calculational method employed) should be their SD amplitude \mathcal{A}_{2L} , with \mathcal{A}_{LD} . In our treatment (see section 2) we have avoided the forbidden low-momentum region by introducing the infrared cut-off Λ of the order of the ρ -mass. We have demonstrated that there is a subtle QCD suppression of the originally quite sizable SD EW 2L amplitude. Therefore, a real $K \rightarrow \gamma\gamma \rightarrow \mu^+\mu^-$ amplitude of a considerable size given in (20) corresponding to low γ -momenta ($\sim \Lambda$ and below), is still allowed. This might be used as a consistency check for the methods of the type employed in Refs. [25, 26].

Taking into account the difficulties inherent to the estimates of the LD amplitude, it is welcome to arrive at the constraint (20). Accordingly, provided the sign of \mathcal{A}_{LD} are correctly given in [4], the BNL experiment combined with the standard-model calculation tends to favour the result of Ref. [26]. In this way, the

scenario of Fig. 2b seems to be preferred by the standard model. Provided that the beyond-standard-model effects are represented by the relatively small SD amplitudes, this scenario hinders the possibility of recovering such effects in the $K_L \rightarrow \mu^+ \mu^-$ decay. The forthcoming data from $K_L \rightarrow \mu^+ \mu^-$ measurements [27] will further test the conclusions of the present paper.

Acknowledgement

Two of us (K.K. and I.P.) gratefully acknowledge the partial support of the EU contract CII*-CT91-0893 (HSMU) and the hospitality of the Physics Department of the Bielefeld University. One of us (I.P.) would also like to acknowledge the hospitality of the Department of Physics in Oslo, and to thank the Norwegian Research Council for a traveling grant.

References

- [1] S.L. Glashow, J. Iliopoulos and L. Maiani, Phys. Rev. D2 (1970) 1285.
- [2] M.K. Gaillard and B.W. Lee, Phys. Rev. D10 (1974) 897; M.K. Gaillard, B.W. Lee and R.E. Shrock, Phys. Rev. D13 (1976) 2674.
- [3] M.B. Voloshin and E.P. Shabalin, JETP Lett. 23 (1976) 107 [Pis'ma Zh. Eksp. Teor. Fiz. 23 (1976) 123].
- [4] A.P. Heinson et al. (BNL E791), Phys. Rev. D51 (1995) 985.
- [5] T. Akagi et al., Phys. Rev. Lett. 67 (1991) 2618.
- [6] L.M. Sehgal, Phys. Rev. 183 (1969) 1511; B.R. Martin, E. de Rafael and J. Smith, Phys. Rev. D2 (1970) 179.
- [7] A.M. Gvozdev, N.V. Mikheev and L.A. Vassilevskaya, Phys. Lett. B274 (1992) 205; Sov. J. Nucl. Phys. 53 (1991) 1030 [Yad. Fiz. 53 (1991) 1682]; hep-ph/9511366.
- [8] A.I. Vainstein, V.I. Zakharov, V.A. Novikov and M.A. Shifman, Yad. Fiz. 23 (1976) 1024 [Sov. J. Nucl. Phys. 23 (1976) 540]; V.A. Novikov, M.A. Shifman, A.I. Vainstein and V.I. Zakharov, Phys. Rev. D16 (1977) 223.
- [9] G. Buchalla, A.J. Buras, Nucl. Phys. B412 (1994) 106; G. Buchalla, A.J. Buras and M.E. Lautenbacher, Rev. Mod. Phys. 68 (1996) 1125; G. Buchalla, hep-ph/9701377.
- [10] R.E. Shrock and M.B. Voloshin, Phys. Lett. B87 (1979) 375.
- [11] J.F. Donoghue and F. Gabbiani, Phys. Rev. D51 (1995) 2187; G. D'Ambrosio and J. Portolés, Nucl. Phys. B492 (1997) 417.
- [12] E.P. Shabalin, Yad. Fiz. 32 (1980) 249 [Sov. J. Nucl. Phys. 32 (1980) 129].
- [13] E.P. Shabalin, ITEP 86-112; B. Guberina, R.D. Peccei and I. Picek, Phys. Lett. B188 (1987) 258; J.O. Eeg, Phys. Lett. B196 (1987) 87.
- [14] J.O. Eeg, K. Kumerički and I. Picek, in preparation.
- [15] A.I. Vainstein, V.I. Zakharov, L.B. Okun', and M. A. Shifman, Yad. Fiz. 24 (1976) 820 [Sov. J. Nucl. Phys. 24 (1976) 427].
- [16] W.A. Bardeen, A.J. Buras and J.-M. Gerard, Nucl. Phys. B293 (1987) 787; A. Pich and E. de Rafael, Nucl. Phys. B358 (1991) 311.
- [17] J.O. Eeg, Phys. Rev. D23 (1981) 2596.
- [18] I. Picek, Nucl. Phys B (Proc. Suppl.) A24 (1991) 101.
- [19] J.O. Eeg and I. Picek, Phys. Lett. B214 (1988) 651.
- [20] J.O. Eeg, B. Nizić and I. Picek, Phys. Lett. B244 (1990) 513.
- [21] A.E. Bergan and J.O. Eeg, Phys. Lett. B390 (1997) 420.
- [22] M.K. Gaillard and B.W. Lee, Phys. Rev. Lett. 33 (1974) 108; G. Altarelli and L. Maiani, Phys. Lett. B52 (1974) 35.
- [23] Particle Data Group, Phys. Rev. D54 (1996) 1.
- [24] G. D'Ambrosio and D. Espriu, Phys. Lett. B175 (1986) 237.
- [25] L. Bergström, E. Massó and P. Singer, Phys. Lett. B249 (1990) 141.
- [26] P. Ko, Phys. Rev. D45 (1992) 174.
- [27] P. Franzini, hep-ex/9512005, Proc. of the 17th International Symposium on Lepton-Photon Interactions, Beijing 1995, World Scientific, Singapore 1996, p. 414.